

# Use of Rietveld refinement for elastic macrostrain determination and for evaluation of plastic strain history from diffraction spectra

M. R. Daymond,<sup>a)</sup> M. A. M. Bourke, and R. B. Von Dreele  
*MLNSC, Los Alamos National Laboratory, New Mexico 87545*

B. Clausen and T. Lorentzen  
*Materials Department, Risø National Laboratory, Roskilde, Denmark*

(Received 10 March 1997; accepted for publication 8 May 1997)

Macrostrain variations in engineering components are frequently examined using neutron diffraction, at both reactors and pulsed sources. It is desirable to minimize the sampling volume in order to maximize the spatial resolution, although this increases the required measurement time. At reactors, macrostrain behavior is inferred from a single lattice reflection (deemed to be representative of the bulk response). At a pulsed source, a complete diffraction pattern is recorded and accordingly it is natural to fit the entire diffraction spectra using a Rietveld [J. Appl. Cryst. **2**, 65 (1969)] refinement. This means that an idealized crystal structure is fit to the measured distorted crystal structure, which includes deviation of the measured lattice reflections from the ideal due to elastoplastic strain anisotropies, which are dependent on the particular lattice reflection (hkl) considered. We show that elastic macrostrains calculated from lattice parameter changes in Rietveld refinements (without accounting for hkl dependent anisotropies) are almost identical to the bulk elastic response and are comparable to the response obtained from a single lattice reflection typically used by practitioners at a steady state source. Moreover good refinements on the complete pattern are obtained with short measurement times compared to what is required for good statistics for single reflections. By incorporating a description of the elastic strain anisotropy expected in cubic materials into the Rietveld code, an empirical prediction of plastic strain history is possible. The validity of these arguments is demonstrated by analysis of a uniaxial tensile load test and a reanalysis of previously reported data taken on a deformed stainless steel ring. The plastic strain predictions compare favorably with a finite element model. © 1997 American Institute of Physics. [S0021-8979(97)04616-1]

## I. INTRODUCTION

The strain fields occurring in components containing macrostresses (often referred to as type I residual stresses) usually vary over length scales comparable to some representative dimension of the component. One experimental technique for profiling macrostrain variation is neutron diffraction,<sup>1-4</sup> where typically sampling volumes ranging from 1 to 100 mm<sup>3</sup> are used. In most cases, where a variation from tension to compression exists, the response of most, if not all, of the individual lattice reflections (hkl) in a polycrystal will follow the macroscopic trend, i.e., while the responses of individual reflections may differ in magnitude they will generally be similar in sense. In many problems in which macrostrains are present, their effects tend to outweigh the microstrain effects. Thus while intergranular effects lead to significantly atypical responses for specific reflections, it is widely accepted that an empirical selection for a suitable plane for macrostrain profiling is one which is little affected by intergranular strains. (We take suitable to mean one from whose response the macroscopic elastic performance can be determined). Indeed, it is on this selection that the efficiency of residual stress measurements at constant wavelength sources relies since it is often impractical to measure multiple reflections.

Of course, the issue of intergranular interactions is fundamental to an understanding of polycrystalline plasticity.<sup>5-8</sup> We shall discuss this work in that context elsewhere.<sup>9-11</sup> Here instead, we will show that by analyzing diffraction data using Rietveld refinement with existing crystal models, we can obtain macrostrain determinations using the obtained lattice parameter that are comparable with the “best” single peak fits. These results are obtained despite the imperfection of the Rietveld fit, which assumes an “undeformed” crystal structure. Moreover, by accounting for elastic strain anisotropy, we can make quantitative predictions of plastic strain history (at least for cubic materials).

The attraction of using Rietveld refinement on pulsed neutron diffraction data is twofold. First, provided a valid macrostrain can be inferred from changes in the lattice parameter, the time for individual measurements can be reduced compared to the situation if individual reflections must be used. This is especially important when the use of small gauge volumes is required. The second attraction is the potential for including physics that describes the overall deformation of the polycrystal in a fashion that is more efficient than separate analysis of individual reflections. In Sec. V, we describe our attempt to do so. At this stage, the procedure only describes the elastic anisotropy of cubic systems, but the results already suggest the potential for incorporating more sophisticated models.

<sup>a)</sup>Electronic mail: mrd@lanl.gov

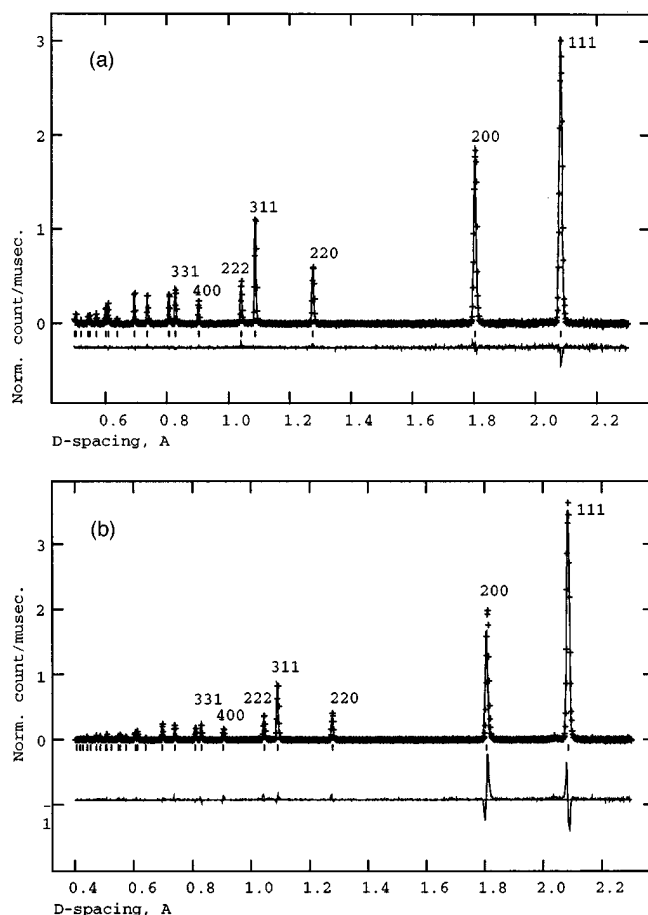


FIG. 1. (a) Diffraction spectrum for stainless steel under a 5 MPa tensile load. The crosses in the top graph show the measured data, and the line through them is the Rietveld fit. The tick marks show the positions of the predicted peaks, and the lower graph is the difference curve (to the same scale as the data). The fitted background response has been subtracted from both the observed and calculated intensities for clarity, and the intensity normalized with respect to the incident spectra. (b) Diffraction spectrum for the same stainless steel sample under a 340 MPa applied load (2% plastic strain). The crosses in the top graph show the measured data, and the line through them is the Rietveld fit. The tick marks show the positions of the predicted peaks, and the lower graph is the difference curve (to the same scale as the data). The fitted background response has been subtracted from both the observed and calculated intensities for clarity, and the intensity normalized with respect to the incident spectra.

## II. RIETVELD REFINEMENT

At a time-of-flight (TOF) source, pulses of neutrons, each of which has a continuous range of velocities and therefore wavelengths, are directed at a specimen. By measuring the flight times of the detected (diffracted) neutrons, their wavelengths can be calculated and diffraction spectra recorded. Implicitly, since the incident spectra are polychromatic, all possible lattice planes in an orientation defined by the fixed detector angle are recorded in each measurement. The scattering vectors for all reflections recorded in one detector lie in the same direction, and thus measure the strain in the same direction. Each reflection is thus produced from a different family of grains, oriented such that the given hkl plane diffracts to the detector. A more complete description of these issues can be found elsewhere.<sup>12</sup>

Typical diffraction spectra for stainless steel under (a) 5 and (b) 340 MPa tensile loads, in the direction of the applied load, are shown in Fig. 1. In addition to fitting the individual lattice reflections, it is possible to perform a Rietveld refinement on the data.<sup>13</sup> If the crystal structure is known, then the intensities and positions of the observed lattice reflections can be predicted. By making a least squares fit between the observed and predicted profiles, the atomic positions and, more importantly in our context, the lattice parameters can be determined. For the discussion that follows, we have used the widely used Los Alamos National Laboratory code written by Larson and Von Dreele, GSAS.<sup>14</sup> Refinements were carried out between 0.358 and 2.4 Å, a total of 35 peaks, using the peak shape function of Ref. 13. Note that for the small uniaxial load [Fig. 1(a)] the refinement, which does not include elastic anisotropy terms, produces an excellent fit, as evidenced by the flat difference curve. This is not the case for the higher load [Fig. 1(b)], where the difference curve indicates shifts in the peak centers relative to the isotropic ideal. The shifts are in opposite senses for the 111 and 200 peaks.

## III. UNIAXIAL TENSILE TEST ON STAINLESS STEEL

Before examining a specimen containing a residual strain field, we performed a series of measurements under uniaxial tensile loading. This allowed us to adjust the applied load and, by using an extensometer, observe the onset of macroscopic plasticity, while simultaneously recording the elastic response of individual reflections. The tensile tests were carried out *in situ* on the Neutron Powder Diffractometer (NPD) at the Manuel Lujan Jr. Neutron Scattering Center at Los Alamos National Laboratory. The load frame used, designed for use in the neutron beam and incorporating universal joints to ensure good uniaxiality of loading, is described elsewhere.<sup>15</sup> Briefly, the loading axis is horizontal and at 45° to the incident beam, allowing simultaneous measurements of lattice plane spacings parallel and perpendicular to the loading direction, in opposing 90° detector banks. Each detector bank comprises 31 individual <sup>3</sup>He tubes that subtend a total of 11°2θ from 84.5° to 95.5°. The spectra from individual tubes are summed together, with suitable corrections for differences in diffraction angle and flight path, to provide a single spectrum for each detector bank.

Stainless steel was selected for this study because of its combination of good scattering properties and relatively large degree of elastic anisotropy. The specimens were fully austenitic (fcc) and had a small rolling texture (<1.5 times random). The material composition was by volume, nominally: Fe 61.64%, Cr 18.25%, Ni 13.42%, Mo 3.66%, Mn 1.48%, Si 0.44%, Co 0.40%, Cu 0.35%, N 0.125% with other elements less than 0.05%. The mean grain size was 28 μm, although some of the grains in the preloaded material showed twinning. The diameter of the gauge section was 8 mm and the volume of material immersed in the neutron beam was ≈ 1000 mm<sup>3</sup>.

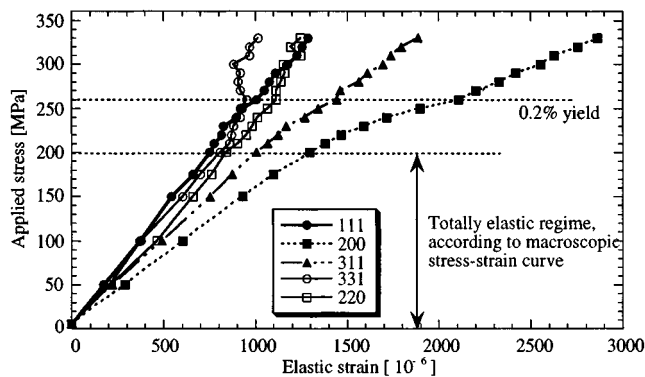


FIG. 2. The change in elastic strain of five lattice planes during a uniaxial tensile test on stainless steel. Lattice plane normals are parallel to the loading direction.

#### IV. CONVENTIONAL RIETVELD RESULTS ON UNIAXIAL LOAD TEST

##### A. Strain by lattice parameter and single peak fits

The anisotropic response of individual lattice reflections during *in situ* loading has been<sup>4</sup> and continues to be the subject of considerable experimental interest. In Fig. 2, the response of the first five lattice reflections are plotted against the applied stress. Also shown is the 0.2% yield limit for plasticity. It is worth reiterating that each line represents the response of a family of grains oriented such that the given hkl lattice plane is parallel to the loading direction. As expected, deviations from linearity of the individual planes occur close to the onset of macroscopic plasticity. Once plastic deformation occurs, the yield of preferentially oriented grains relative to their neighbors causes strain redistribution, and a divergence from the hitherto linear response.

At a TOF source, since all lattice planes are recorded it is natural to attempt a Rietveld refinement. This produces a lattice parameter which is an average over all lattice planes oriented to a specific  $2\theta$ . In the simplest case of a powder or a “truly” strain-free polycrystal, the determination of the lattice parameter is unambiguous. However a problem in interpretation arises when a refinement is performed on a loaded specimen. For example, in Fig. 2, the elastic strain for different reflections clearly diverges as the load is increased. Thus even if a perfect face centered cubic structure was appropriate in the unloaded state (see Fig. 1), it is no longer rigorously correct after a load is applied [Fig. 1(b)].

However, in all cases that we have encountered to date, the elastic strains associated with residual or even applied loads are small enough that a refinement will succeed despite the fact that the diffracted data really represents a distorted crystal structure. Since the validity of using lattice parameters (determined from such refinements) as a suitable determination of residual strain has been argued, our first objective was to compare the results of Rietveld fits with those obtained from individual planes.

Figure 3(a) shows the stress-strain response of three lattice planes, the Rietveld fits, and the macroscopic Young's modulus. The 200 and 111 lattice planes represent the extremes of elastic stiffness in a cubic material with the 311 lying approximately halfway between ( $A_{111}=0.333$ ,  $A_{200}$

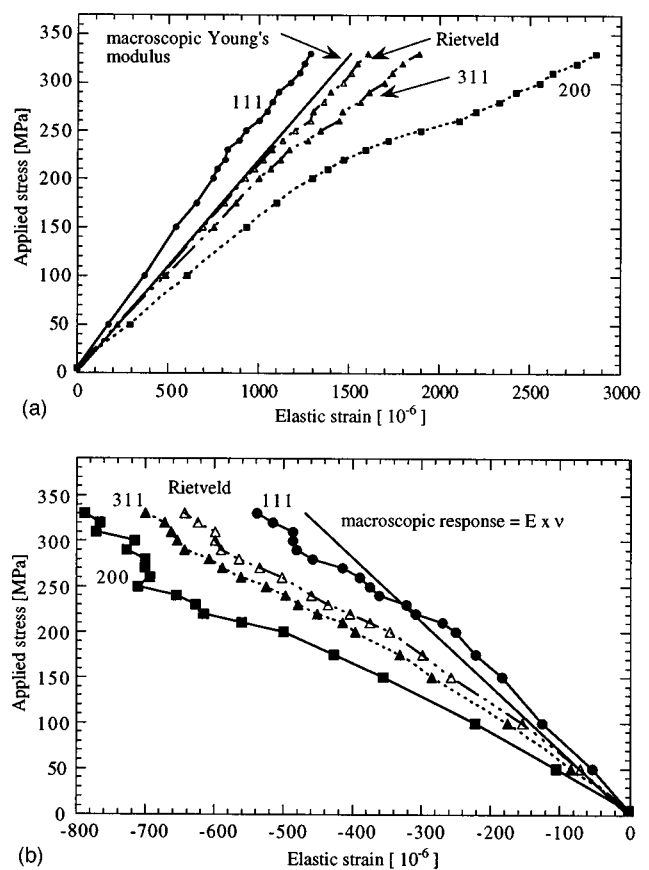


FIG. 3. (a) The stress-strain responses of the 111, 200, and 311 planes, parallel to the load axis, compared with strains (determined from the lattice parameter) of a conventional (i.e., not using elastic anisotropy terms) Rietveld refinement. Also shown is the bulk elastic response, i.e., gradient equal to the Young's modulus. (b) The stress-strain responses of the 111, 200, and 311 planes perpendicular to the load axis, compared with strains (determined from the lattice parameter) of a conventional (i.e., not using elastic anisotropy terms) Rietveld refinement. Also shown is the bulk elastic response, i.e., gradient equal to the Young's modulus multiplied by the Poisson's ratio.

$=0$ , and  $A_{311}=0.157$ ; see Sec. V). The 311 is considered to be one of the planes in stainless steel least effected by inter-granular strains, and is commonly used at reactors for residual strain profiling.<sup>16</sup>

The agreement of the Rietveld result with the macroscopic gradient is good for the axial direction [Fig. 3(a)], especially in the elastic region. If we consider a linear elastic response as ideal (see discussion below) and fit a linear response to the purely elastic part of each curve, then the deviations of the actual strains from an extrapolated elastic line at the maximum load can be determined. The maximum fractional differences at 340 MPa ( $\approx 2\%$  plastic strain) for the 111, 311, 200, and Rietveld are: 7.5%, 10.6%, 26.7%, and 6.0% ( $\pm 0.1\%$ ), respectively. Surprisingly, the 111 shows a smaller difference in the sense of maximum deviation from a linear elastic response, than does the 311. In a single peak measurement of strain, it is usual to determine macroscale stresses through the use of an experimentally determined diffraction elastic constant, and these percentage values thus suggest the level of error which might be involved with this approach.

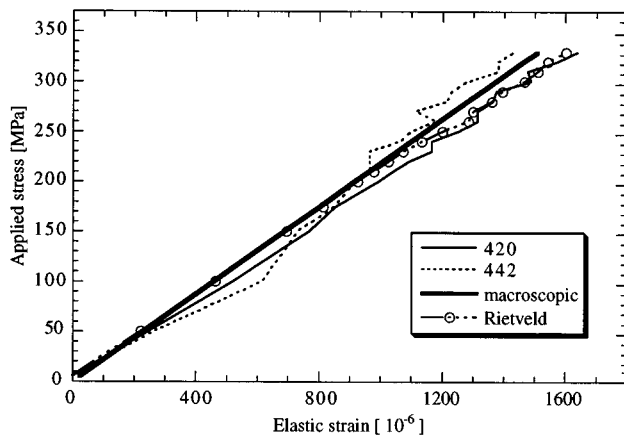


FIG. 4. The stress-strain response of the 420 and 442 peaks determined by single peak fits, compared with the Rietveld fitting method (planes parallel to loading direction). The macroscopic elastic stress-strain slope is shown for comparison.

In fact, of the 15 highest  $d$  spacing peaks—all that it was possible to do reasonable single peak fits for—the best single peaks, both in terms of agreement with the macroscopic modulus and which showed least deviation from linearity, were the 420 and 442 (Fig. 4). Due to the poorer intensities of these higher order peaks however, the obtained responses contain a larger scatter.

In the transverse direction [Fig. 3(b)], smaller total strain changes are observed than in the axial direction, resulting in a proportionately larger scatter in the strains. None the less, the response of the individual peaks and Rietveld calculated strain is approximately linear until the start of yielding, at around 200 MPa. The transverse Rietveld gradient is slightly different from the macroscopic response in the elastic regime, and this difference is accentuated once plasticity occurs. This may be due to the use of an incorrect reference value of the Poisson's ratio to determine the macroscale stress-strain response, whereas the modulus in Fig. 3(a) was experimentally determined during the load test.

## B. Effect of reduced count time on lattice parameter

In Fig. 3(a), the Rietveld determined elastic response is close to the bulk material response, and remains approximately linear in the macroscopically plastic regime. This, it can be argued, is at least as good as any single peak measurement for gauging residual macrostrains. From an efficiency standpoint, this is significant, because a converged Rietveld refinement can be achieved far more quickly than a single peak fit, on pulsed source data. The dramatically reduced count times are possible because the refinement uses diffraction data across a wide  $d$  spacing range down to small (0.3 Å) spacings. Since overlapped reflections contribute as much to the refinement as do separated reflections at larger  $d$  spacings, this makes more efficient use of the TOF spectra than if only the large  $d$  spacing reflections are considered. It also suggests why the results might agree well with the bulk elastic response.

To examine the count time issue, we revisited the data in Fig. 3(a), but instead of using a spectrum summed over the

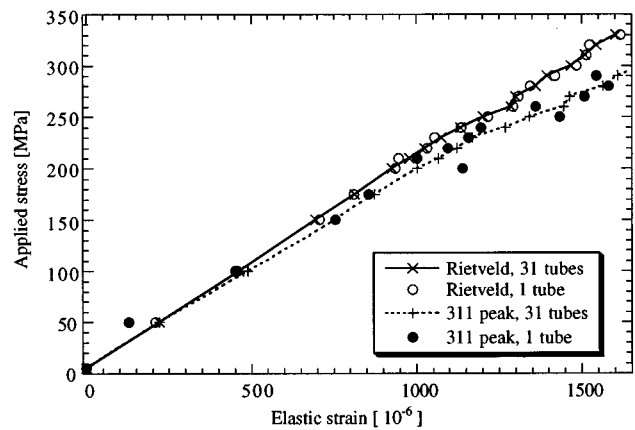


FIG. 5. The stress-strain response obtained parallel to the loading direction for Rietveld and for a single peak fit to the 311 plane, showing the effect of reduced counting statistics.

31 tubes (that comprise the detector bank) we considered a single tube, which to a first approximation is like using the complete detector for 1/31 of the time. Since each detector has a finite angular range ( $11^\circ$ ), we chose to use the central tube, since the strain obtained from this tube's data will represent the strain parallel, or perpendicular, to the loading direction. Selection of any other single detector would represent a slightly off-axis measurement. Figure 5 shows the results of the Rietveld strain, and the 311 reflection for the single tube and complete detector. The difference in the Rietveld determined strain for the reduced counting statistics is negligible, whereas for the single peak fit it is considerably poorer. While this does not necessarily imply that the same macrostrain result could have been inferred 31 times faster than was the case in Fig. 3(a) (due to the different contributions from time dependent and independent noise in the data acquisition electronics), it does show the great improvement in counting times that can be obtained by using a Rietveld analysis.

## V. ELASTIC ANISOTROPY FACTOR IN THE RIETVELD REFINEMENT—UNIAXIAL LOAD TEST

In its simplest implementation, the problem with the Rietveld description is that it does not account for the elastic or plastic anisotropies present in polycrystalline materials under load (even though as shown above it does provide a good empirical bulk average). Describing the elastic divergence of the various planes, at least in the elastic regime, is a first step to including more subtle descriptions of polycrystalline deformation. For a cubic crystal, the single crystal plane specific modulus,  $E_{hkl}$  can be expressed as<sup>17</sup>

$$1/E_{hkl} = S_{11} - 2(S_{11} - S_{12} - 1/2S_{44})A_{hkl}, \quad (1a)$$

where  $S_{ij}$  is the single crystal compliance tensor in collapsed matrix notation and

$$A_{hkl} = (h^2k^2 + h^2l^2 + k^2l^2)/(h^2 + k^2 + l^2)^2 \quad (1b)$$

and thus has limiting values of  $A_{h00} = 0$  and  $A_{hhh} = 1/3$ .

Taking this into account, we introduced a fitting parameter,  $\gamma$ , into the Rietveld fit that shifts the position of each peak from a perfect cubic structure by a quantity propor-

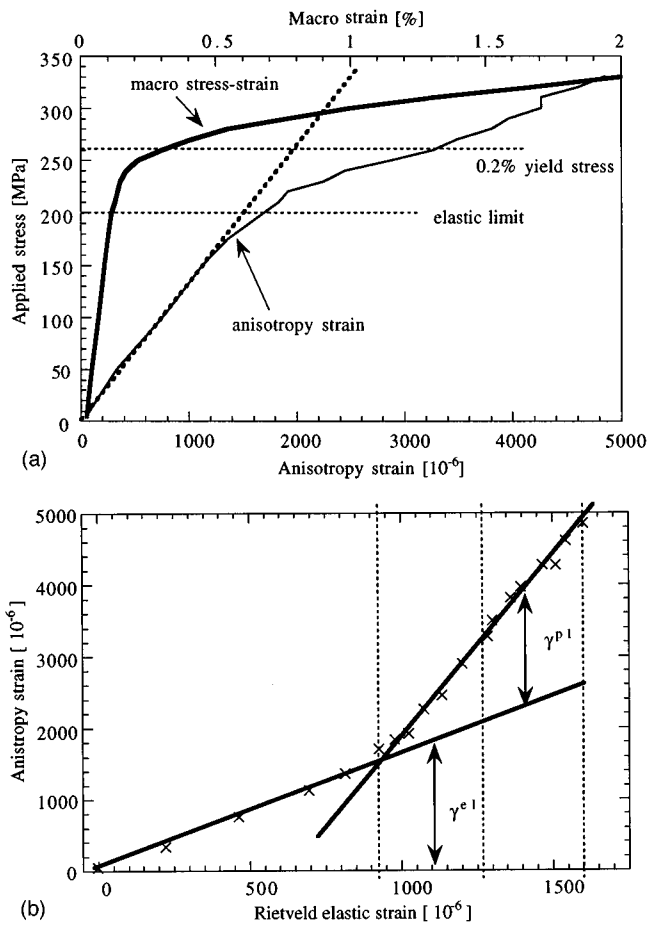


FIG. 6. (a) The variation of anisotropy factor with applied stress, superimposed with the stress-strain relationship. (b) Variation of anisotropy factor with internal phase strain as determined by Rietveld fit. Straight solid lines indicate the division of the anisotropy factor into two components. The vertical broken lines indicate the elastic strains correlating with macroscopic plastic strains of 0%, 0.2%, and 2%, respectively.

tional to  $\gamma A_{hkl}$ . Accordingly, the refinement is modified so that the lattice parameter now tracks a nominal  $h00$  direction, and the other reflections are anisotropically strained according to

$$\epsilon_{hkl} = \epsilon_{h00} - (\gamma A_{hkl}/C), \quad (2)$$

where  $\epsilon_{hkl}$  is the strain of a particular reflection ( $\mu\epsilon$ ). In GSAS,  $\gamma$  represents the peak position offset in  $\mu s$ , and  $C$  is the diffraction constant for the instrument (see Ref. 13).

In the elastic regime, the parameter  $\gamma$  should correlate solely with the elastic anisotropy and therefore, from Eq. (1), we expect it to be proportional to the applied stress. However, in the plastic regime, it will, at best, give a qualitative improvement to the fit, and its validity will depend on the range and magnitude of the  $hkl$  dependent differences. Figure 6(a) shows the anisotropy strain ( $\gamma/C$ ) plotted against the applied stress, with the macrostress-strain curve superimposed. (Note that the maximum correction to an  $hkl$  reflection would be  $1/3$  of the anisotropy strain). The qualitative similarities between the two graphs are striking. Initially the anisotropy strain increases monotonically then, at the onset of plasticity, it changes slope. Figure 6(b) shows ( $\gamma/C$ ) plotted against the elastic strain predicted using a Rietveld fit

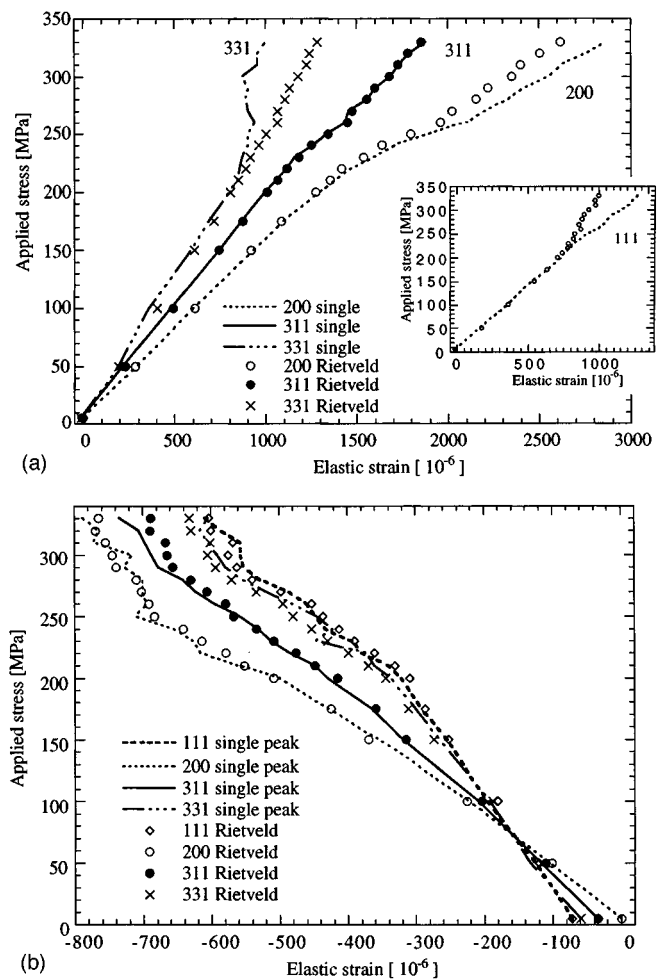


FIG. 7. (a) The strain response in the axial direction of the 200, 311, 331, and 111 planes (1) as determined by single peak fits (lines), and (2) as calculated from the Rietveld fit using the anisotropy factor  $\gamma$  (points). For clarity, the 111 planes are shown in the insert. The absolute values of strain for the single peak fits at zero stress have been shifted to agree with the Rietveld predictions. (b) The strain response in the transverse direction of the 200, 311, 331, and 111 planes (1) as determined by single peak fits (lines), and (2) as calculated from the Rietveld fit using the anisotropy factor (points). The absolute values of strain for the single peak fits at zero stress have been shifted to agree with the Rietveld predictions.

that does not use the anisotropy factor [i.e., an approximately linear applied stress-internal strain relation, c.f. Fig. 3(a)]. The slope discontinuity in Fig. 6(b) occurs between 900 and 1000  $\mu\epsilon$ , which correlates well with the onset of plasticity in Fig. 3(a).

We postulate that  $\gamma$  can be separated into two contributions; an elastic component  $\gamma^{el}$  and a plastic component  $\gamma^{pl}$ , where  $\gamma = \gamma^{el} + \gamma^{pl}$ . An examination of these two figures [6(a) and 6(b)] suggests that  $\gamma^{el}$  is proportional to the elastic Rietveld strain, and that  $\gamma^{pl}$  can be described as a function of the macroscopic plastic strain. Note that we have not included any physics to describe the changes in partitioning of strain between reflections due to plasticity (most obviously illustrated by the nonlinear response of the 200 reflection in Fig. 3).

In addition to the evolution of  $\gamma$ , we can also use Eq. (2) to predict the  $hkl$  strains in the modified Rietveld, i.e., given the Rietveld lattice parameter strain ( $\epsilon_{h00}$ ) and the value of

$\gamma$ , we can calculate  $\epsilon_{hkl}$ . These can be compared with measured single peak fits. Figure 7(a) shows the strain response of four lattice planes determined both by single peak fits, and using the Rietveld fit incorporating the anisotropy factor, parallel to the loading direction. In the elastic regime (stress < 210 MPa), excellent agreement is achieved for all the reflections shown. However, deviation from the elastic response occurs above 210 MPa, and is in opposite senses for the 200 and 311 planes. It is to be expected that the Rietveld refinement should still give an average of the response of the individual planes, but this fact also indicates the complexity of the plastic anisotropy behavior. Interestingly, the 311 response predicted by the Rietveld now tracks exactly with the single peak measured value! This suggests that it is probably a good representation of the average response of the planes. It is also interesting to note that the 111 plane (inset) shows a considerable difference between the modified Rietveld and single peak in the plastic regime, suggesting that the elastic anisotropy model is not capturing the behavior of the 111 plane very well in the plastic regime. This is because the 111 has actually remained approximately elastic, as stated before, yet our model will still ascribe the largest shift to this peak relative to the  $\epsilon_{h00}$  peak (since  $A_{111} = 1/3$ ).

The single peak strains shown in Fig. 3 were determined by assuming that the lattice parameters obtained at zero stress were, for each plane, stress-free. However, the Rietveld results in Fig. 7(b) suggest that even in the macroscopically unstressed state there are residual intergranular strains present, which are particularly clear in the transverse direction. In fact, these strains are small, particularly considering the method by which they have been determined. In order to make comparisons however, the single peak strains at zero stress have been shifted to agree with the Rietveld predictions, for both axial and transverse data. The correlation between Rietveld predictions and single peak values at higher stress levels is then excellent. In fact, the absolute strain values will still not be totally correct, since we have now made the assumption that the 200 plane is strain-free at zero stress, since it is the Rietveld determined lattice parameter, whereas it is more likely from a stress balance argument that one of the intermediate planes will be strain-free, with the 200 plane thus in tension, and the 111 plane in compression. These anisotropy strains, presumably present due to the deformation the specimen has undergone during processing, are in the opposite sense of those produced by the Poisson anisotropy strains due to the applied load, and thus the transverse direction shows zero anisotropy at an applied stress of  $\sim 65$  MPa.

## VI. APPLICATION TO A COMPRESSED RING CONTAINING A RESIDUAL STRESS FIELD

### A. Ring description

In the uniaxial load test described above, the applied stress and macroscopic material response were known. However, to test the Rietveld refinement on a residual strain problem and to investigate the possibility of predicting plastic strain using our  $\gamma^p$  formulation, we revisited data collected on a compressed ring, which has been examined at the Los

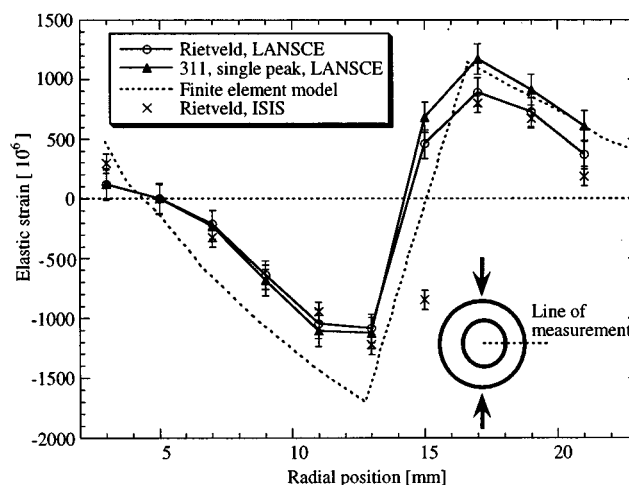


FIG. 8. The tangential elastic strain determined using Rietveld and single peak (311) analysis of neutron diffraction data, compared with FE calculations, as a function of distance from inner radius. Insert shows the ring, and position of the measurement line.

Alamos Neutron Scattering Center (LANSCE), at the ISIS facility (UK) and at the Chalk River Laboratory (Canada). At the three facilities, the gauge volume was similar in size with the significant dimension being typically 2 or 3 mm. The original results and description of the ring have been published<sup>18</sup> and only a brief description is included here. The ring was made from fully austenitic stainless steel, with an internal diameter=76 mm, external diameter=127 mm, and thickness=13 mm. The mean grain size was 25.3  $\mu\text{m}$ , and the composition was nominally by volume Fe 64%, Cr 21%, Mn 9%, Ni 6%. The material has an approximately random texture. The ring was compressed by 3.4 mm along a diameter, sufficient to induce plastic deformation, at which point the load was removed, leaving a residual strain distribution. Here we report only the tangential strains, measured at the position indicated in Fig. 8 insert. The deformation was modeled by finite element (FE) analysis using two-dimensional, second-order plane stress elements. (Previous work indicated that little difference in the numerical results were obtained by using a three dimensional mesh).<sup>18</sup>

### B. Macrostrain distribution predictors

The deformation of the ring produces a predictable macroscopic strain distribution across the radius, as shown in Fig. 8. The FE values (averaged over a sampling volume comparable with LANSCE and ISIS experiments) use the macroscopic stiffness, i.e., they do not account for individual plane stiffness. Shown in Fig. 8 are; the LANSCE measured 311 single peak response, and the LANSCE and ISIS (data collected on ENGIN) Rietveld (no  $\gamma$ ) strains determined from the lattice parameters. Apart from the ISIS measurement at 15 mm there is good agreement between the experimental data sets. In view of differences in the setup at LANSCE and ISIS, the agreement is as good as can be expected.

The disparity with the FE calculation may arise from the oversimplified bilinear plastic hardening law used in the model. This resulted in too plastic a system, as indicated by the final macroscopic displacement (after unloading) being

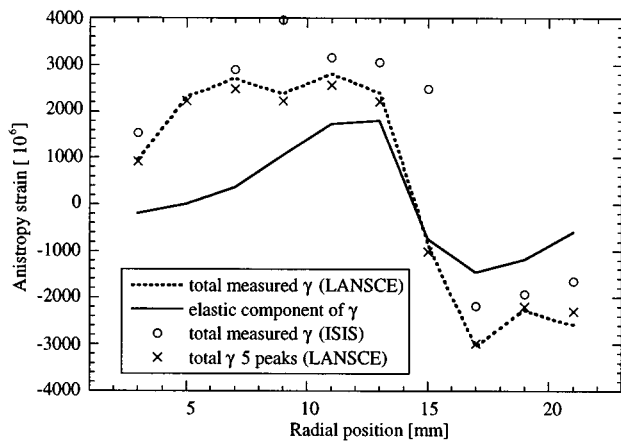


FIG. 9. Variation of anisotropy strain with radial position, showing (1) anisotropy strain measured at LANSCE, (2) the anisotropy strain calculated from the elastic strain measurements, (3) the anisotropy strain determined from the ISIS measurements, (4) the anisotropy strain determined from using only the five highest  $d$  spacing peaks of the LANSCE data.

2.8 mm in the model, compared to 2.6 mm experimentally, despite deformation to the same (loaded) strain.

### C. Variation of $\gamma$ and plastic strain prediction

In Fig. 6(b), the change in response of  $\gamma$  at the onset of plasticity raises the possibility of using it as an indicator of plastic history. Accordingly, we repeated the Rietveld refinements on the ring spectra collected at LANSCE and plotted the anisotropy strain versus the radial position in Fig. 9. Using the elastic strains from a Rietveld refinement (not including  $\gamma$ ) on the ring (Fig. 8), and the relationship between  $\gamma^{\text{el}}$  and elastic strain determined in the tensile test [Fig. 6(b)], the elastic component of the anisotropy ( $\gamma^{\text{el}}$ ) in the ring was determined. This is indicated by the solid line in Fig. 9. There is a clear discrepancy between this and the total measured anisotropy ( $\gamma$ ), shown by the broken line.

Also shown in Fig. 9 are comparable results obtained at ISIS (circles). The similarity of the two sets of results is reassuring and suggests that the observed anisotropy factor is a true material characteristic, and not some function of the fitting, dependent on instrument properties.

In the following discussion, we assume that the relationship between strain and anisotropy is symmetric with respect to tension and compression, for both elastic and plastic strains. Accordingly, if we make the assumption that the difference between the measured  $\gamma$  and the  $\gamma^{\text{el}}$  predicted from the Rietveld elastic strain, as shown in Fig. 9, is due to plasticity, and then use the  $\gamma^{\text{pl}}$  as a function of macroscopic plastic strain, which was obtained from the uniaxial tension test [Fig. 6(b)], the macroscopic plastic strain in the ring can be predicted. Note that we are “calibrating” our plastic anisotropy behavior using a tensile test on stainless steel of a nonidentical, though fairly similar, grade to that used in the compressed ring. These calculated plastic strains are compared with the FE predictions in Fig. 10. The error bars are estimates obtained by examining the sensitivity of the anisotropy factor to the number of peaks used in the refinement. The agreement is good, especially since the tensile specimen

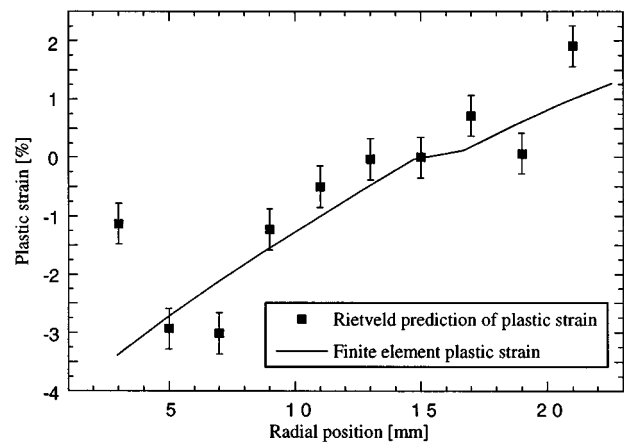


FIG. 10. The predicted plastic strains from the Rietveld analysis, compared with those determined using the finite element model, as a function of distance from the inner radius.

and ring are not identical production route materials, and there are differences in the elastic strain distribution (Fig. 8), which we have suggested are, at least in part, due to the simplicity of the model used in the FE. Thus it is possible to use an estimate of  $\gamma^{\text{pl}}$  to make quantitative predictions of the plastic strain history, even in the absence of a rigorous description of the polycrystalline interactions.

## VII. DISCUSSION

Often the principle aim of a neutron diffraction macrostrain measurement is to give an engineer something useful, in terms of understanding areas of high internal stress or validation of a (usually) continuum mechanics model prediction. It is frequently true that the macroscopic strain variations are treated as the most important part of the answer partly because they usually dominate the microstrain effects, and partly because the microstrain aspects cannot at this time be easily coupled to mechanical property predictions. Whether or not this is true, we must somehow define a “goodness” for a method of strain calculation, whether it be the choice of a specific  $hkl$  for a single peak fit or the validity of a Rietveld refinement.

Typically numerical predictions, such as those using the finite element method, utilize continuum models of material behavior. The input characteristics of the materials in the models are obtained from simple uniaxial loading or creep tests. In this context, one might advocate that the most suitable test of a diffraction determined strain (which by definition is the elastic component of the total strain) is, first how little deviation from the linear elastic response occurs in the plastic regime, and second how well it compares with the macroscopic elastic gradient, i.e., the Young’s modulus of the sample. According to these criterion, the basic Rietveld refinement (without  $\gamma$ ) is highly effective. In fact, while the requirement of agreement with macrostiffness is not rigorous (provided the effective polycrystalline stiffness of an individual plane is known), it is advantageous because the bulk elastic response is, if not known, easier to determine than a plane specific elastic modulus.

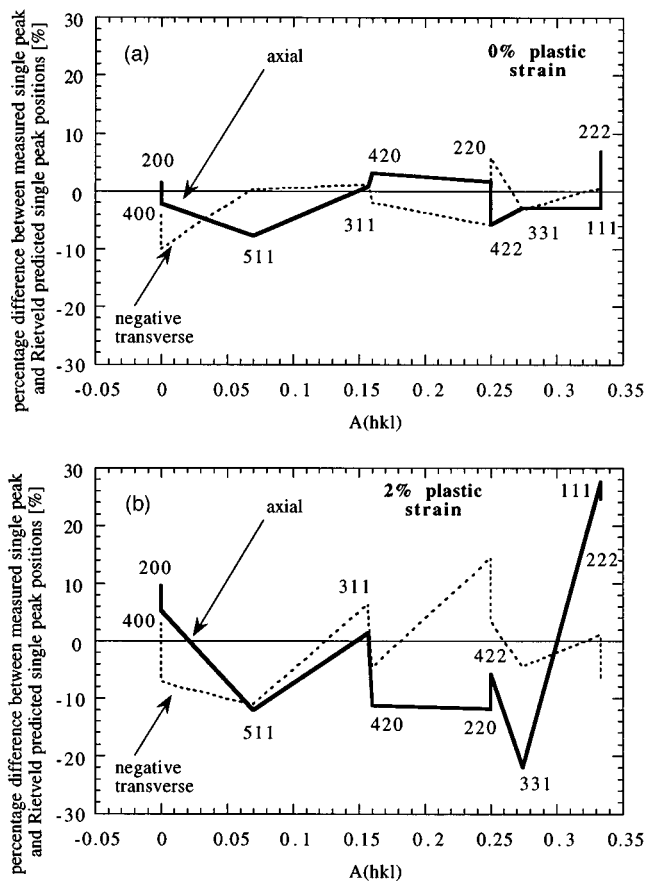


FIG. 11. (a) The percentage difference between single peak fit and Rietveld prediction of single peak response for an applied load of 150 MPa (0% plastic strain); (Single peak strain—Rietveld predicted single peak strain)/Rietveld predicted single peak strain. The axial response is shown with a continuous line, the negative transverse with a broken line (shown negative to highlight the similarities between transverse and axial response). (b) The percentage difference between single peak fit and Rietveld prediction of single peak response for an applied load of 330 MPa (2% plastic strain); (Single peak strain—Rietveld predicted single peak strain)/Rietveld predicted single peak strain. The axial response is shown with a continuous line, the negative transverse with a broken line (shown negative to highlight the similarities between transverse and axial response).

The difference between the Rietveld predicted single peak strains (i.e., obtained using the anisotropy factor) and the single peak strains can be seen more clearly in Fig. 11. The percentage differences for each of the first ten diffraction peaks are shown for (a) 150 (elastic regime) and (b) 340 MPa (2% plastic strain) applied loads. In the elastic regime [Fig. 11(a)], the percentage difference is small. In fact, the absolute magnitudes of the differences are here of the order of  $50 \mu\epsilon$  or less, which is comparable to the measurement uncertainty and explains why no clear trends can be seen. In the plastic regime however [Fig. 11(b)], both compressive and tensile differences are clearly seen, and the good fit of the 311 plane is shown again. Interestingly, there is a strong qualitative inverse correlation between the transverse and axial responses. The mean absolute difference observed in Fig. 11(b) is of the order  $250 \mu\epsilon$ .

In our attempt to capture the strain anisotropies inherent in this elastically (and plastically) anisotropic material,  $\gamma$  does well in the elastic regime but fails to fully capture the

behavior of the individual planes in the plastic regime (Fig. 7). This is unsurprising due to the simplicity of the approach. Nevertheless it does improve the refinement and qualitatively identifies the onset of plasticity.

The use of the anisotropy factor allowed the identification of initial residual strains, i.e., the presence of intergranular strains even in the nominally unloaded material. These are presumably present due to the rolling history of the samples. With this assumption, good agreement is obtained at higher applied loads, which, along with the improved Rietveld fit obtained, suggests that these are real effects. This information could not be easily obtained using the single peak analysis where a nominally unstrained initial state must be assumed.

This Rietveld implementation is not restricted to TOF sources, since it requires only the monitoring of a representative set of lattice planes. Of course, the Rietveld refinement results will be a “compromise” fit which will depend on the range of reflections in the fit, as well as the resolution behavior of the instrument over these reflections. However, our work suggests that in this system, considering only the top 5 (largest lattice spacing) peaks captures most of the behavior of the anisotropy factor (Fig. 9). The top five peaks show the highest intensity, normalized with respect to the incident spectra, and therefore might be expected to have a larger effect on the overall response. This is compensated for in the Rietveld fit however, through the use of a weighting function which is inversely proportional to the variance of the counting statistics.<sup>13,14</sup> For a large number of counts, the variance will be approximately the number of counts (since the standard deviation  $\sigma \approx \sqrt{N}$ ), i.e., the intensity. The effect of this weighting is therefore to normalize the least squares fit with respect to intensity, i.e., to “level” the contribution of the peaks. It should be noted that the lower order planes tend to show a higher degree of anisotropy, in terms of the magnitude of shifts in strain. The removal of the higher order planes none the less seems to have a relatively small effect on the observed anisotropy. In cases where a more complex strain field exists, this may not be the case. On the other hand, if the Rietveld model fits the observed behavior and correctly captures the physics, as it seems to in the elastic regime at least, then it can be argued that it does not matter how many reflections are used in the fit, provided that a minimum number is used which covers the whole range of observed responses, and allows the required parameters to be determined.

One reason for pursuing the use of Rietveld refinements concerns the increasing complexity of engineering materials. With the increasing prevalence of lower symmetry crystal structures or microstructurally complex systems containing two or three phases, nonoverlapped lattice reflections are hard to find. In these situations, the use of a Rietveld refinement, even if it is only for a few reflections easily measured at a reactor source, has clear advantages. While the current implementation of  $\gamma$  is only valid for a cubic material, there is no *a priori* reason why it should not be possible to accommodate more complex crystal structures, although the functions describing the reciprocal of planar stiffness will be more complicated and will therefore require more than one

fitting parameter. Ultimately it should also be possible to build more subtle models of polycrystalline deformation into code. Clearly further work needs to be performed but the current indicators are good. For instance, the effect of a high degree of texture on the behavior of the anisotropy factor needs to be examined, and is the subject of current research.

## VIII. CONCLUSIONS

Conventional Rietveld refinements were made on neutron diffraction data, collected at a series of loads, during a uniaxial tensile test of an austenitic stainless steel, throughout the elastic region up to a plastic strain of 2%. The response of the lattice parameter agreed well with the expected bulk elastic response—even in the plastic region. Indeed it does so, as well as any of the individual reflections, demonstrating that the refinement is a good empirical averaging procedure across the various hkl responses. Moreover a refinement from which meaningful ( $50 \times 10^{-6}$  accuracy) elastic strain variations can be determined, can be achieved in times far shorter than would be needed for comparable accuracies in individual reflections on a pulsed neutron source.

A strain anisotropy factor,  $\gamma$ , has been implemented into the Los Alamos National Laboratory Rietveld code GSAS. It allows the elastic anisotropic hkl response for cubic materials to be approximated. For the load test in the elastic region, the Rietveld predicted single peak responses are in excellent agreement with the measured values. The response of  $\gamma$  undergoes a discontinuity at the onset of plasticity. We postulate that  $\gamma$  can be deconstituted into an elastic and a plastic component. Using this idea, with calibration from the uniaxial load test, the plastic strain history of a deformed ring was predicted with reasonable agreement with a finite element calculation.

## ACKNOWLEDGMENTS

The Manuel Lujan Jr. Neutron Scattering Center is a national user facility funded by the United States Department

of Energy, Office of Basic Energy Science, and Defense Programs. This work was supported in part by DOE Contract No. W-7405-ENG-36. The authors would like to acknowledge Elane Flower, Tom Holden, Joyce Roberts, and John Wright all of whom were involved with the measurements on the deformed ring. We would also like to thank Ning Shi for many useful discussions.

- <sup>1</sup>H. M. Rietveld, *J. Appl. Crystallogr.* **2**, 65 (1969).
- <sup>2</sup>H. J. Prask and C. S. Choi, *J. Nucl. Mater.* **126**, 124 (1984).
- <sup>3</sup>M. T. Hutchings, *Nondestr. Test. Inst.* **5**, 395 (1990).
- <sup>4</sup>A. J. Allen, M. A. Bourke, W. I. F. David, S. Dawes, M. T. Hutchings, A. D. Krawitz, and C. G. Windsor, *Effects of Elastic Anisotropy on the Lattice Strains in Polycrystalline Metals and Composites Measured by Neutron Diffraction at ICRS 2 at Nancy* (Elsevier, London, 1989), pp. 78–83.
- <sup>5</sup>G. I. Taylor, *J. Inst. Metall.* **62**, 307 (1938).
- <sup>6</sup>R. Hill, *J. Mech. Phys. Solids* **13**, 89 (1965).
- <sup>7</sup>G. R. Canova, U. F. Kocks, C. N. Tomé, and J. J. Jonas, *J. Mech. Phys. Solids* **33**, 371 (1985).
- <sup>8</sup>R. J. Asaro and A. Needleman, *Acta Metall.* **33**, 923 (1985).
- <sup>9</sup>B. Clausen, T. Lorentzen, and T. Leffers (unpublished).
- <sup>10</sup>B. Clausen and T. Lorentzen (unpublished).
- <sup>11</sup>B. Clausen, Ph.D. thesis Risø-R-985 (EN), Risø National Laboratory, 1997.
- <sup>12</sup>M. A. M. Bourke, J. A. Goldstone, and T. M. Holden, in *Measurement of Residual and Applied Stress Using Neutron Diffraction*, edited by M. T. Hutchings and A. D. Krawitz (Kluwer, Dordrecht, 1992), NATO ASI Series E No 216, pp. 369–382.
- <sup>13</sup>R. B. Von Dreele, J. D. Jorgensen, and C. G. Windsor, *J. Appl. Crystallogr.* **15**, 581 (1982).
- <sup>14</sup>A. C. Larson and R. B. Von Dreele, Report No. LAUR 86-748, Los Alamos National Laboratory, 1994.
- <sup>15</sup>M. A. M. Bourke, J. A. Goldstone, N. Shi, J. E. Allison, M. G. Stout, and A. C. Lawson, *Scr. Mater.* **29**, 771 (1993).
- <sup>16</sup>T. M. Holden (personal communication).
- <sup>17</sup>J. F. Nye, *Physical Properties of Crystals* (Oxford University Press, Oxford, 1992).
- <sup>18</sup>T. M. Holden, B. R. Hosbons, S. R. MacEwen, E. C. Flower, M. A. Bourke, and J. A. Goldstone, in *Measurement of Residual and Applied Stress Using Neutron Diffraction*, edited by M. T. Hutchings and A. D. Krawitz (Kluwer, Dordrecht, 1992), NATO ASI Series E No 216, pp. 93–112.